Animal Microbiome

RESEARCH

Open Access

Microbial diversity and pigment synthesis in the accessory nidamental gland: species-specific and color-associated patterns in bigfin reef squid (*Sepioteuthis lessoniana*)

Ling Chiu[1,2], Jei-Lin Guo[3], Hau-Wen Li[3], Hai-Jin Chang[4], Shan-Hua Yang[4], Sylvie Dufour[5], Ching-Fong Chang[6], Yung-Che Tseng[2*] and Guan-Chung Wu[3,6*]

Abstract

Background In certain cephalopod species, two distinct symbiotic organs host large populations of microorganisms: the light organ, regulated by the daily cycle, and the accessory nidamental gland (ANG), regulated by the female reproductive cycle. While host-microbiota interactions in the light organ of the bobtail squid are well understood, the dynamics within the ANG remain largely unexplored. This study uses the bigfin reef squid, *Sepioteuthis lessoniana*, as a model to investigate the microbiomes associated with specific regions of the ANG, capitalizing on its relatively large gland size compared to the bobtail squid. Our goal was to characterize species-specific microbiomes in the ANG and explore how pigmented region-dependent microbes contribute to reproductive fitness in bigfin reef squid.

Results Histological results indicate that four types of epithelial cells were observed in the secondary tubules of inner ANG layer. Using an amplicon-based approach, we found that *Alphaproteobacteria* were highly abundant in different cephalopod species. Beta diversity analyses revealed significant interspecies differences in microbiomes, while alpha diversity showed that the bigfin reef squid harbored a richer bacterial community than the other two species. Notably, pigmented regions of the ANG exhibited lower microbial diversity compared to whole ANG tissues, with *Alphaproteobacteria* significantly enriched in these regions. *Hyphomicrobiaceae* (*Alphaproteobacteria*) were unique to the orange regions, while *Fodinicurvataceae* (*Alphaproteobacteria*) and *Flavobacteriaceae* (*Bacteroidia*) were exclusive to the white regions. qPCR results showed higher transcription levels of immune response-associated genes in the orange region compared to other pigmented regions, suggesting localized immune interactions.

Conclusions These findings suggest that *Alphaproteobacteria*, particularly the *Hyphomicrobiaceae* clade, may correlated to the synthesis orange pigmentation in the ANG of the bigfin reef squid. The roles of *Hyphomicrobiaceae* in ANG symbiosis and reproductive fitness still needs further investigation. With this knowledge, we propose further investigations using in situ hybridization to detect host-expressed genes and pigmented region-dependent bacteria

*Correspondence:
Yung-Che Tseng
yctseng@gate.sinica.edu.tw
Guan-Chung Wu
gcwu@mail.ntou.edu.tw

Full list of author information is available at the end of the article

as markers. This approach will facilitate the study of localized host-microbiota interactions in distinct pigmented regions of the ANG, providing deeper insights into the mechanism of host-microbe communication.

Keywords Female reproductive organ, Microbiome, 16S rRNA amplicon, Symbiosis, Cephalopod, *Hyphomicrobiaceae*

Background

In some cephalopods, large populations of microorganisms are often found in specialized organs, such as the light organ and the female reproductive organ known as the accessory nidamental gland (ANG) [1]. While mechanisms for the selection and maintenance of symbiotic luminescent *Vibrio fischeri* in the light organ of the Hawaiian bobtail squid (*Euprymna scolopes*) are well described (reviewed in [2]), comprehensive studies on the bacterial selection and maintenance mechanisms in the ANG during female maturation are still lacking.

In female cephalopods, the glandular system, including oviduct glands and nidamental glands, is involved in forming various egg membranes, known as egg capsules [3]. Microbiota in the ANG is transferred from the mother to the egg capsule via jelly-like secretions from the nidamental gland during egg capsule formation [4]. These ANG-derived bacteria are crucial for embryonic survival, as they prevent fungal fouling on the egg capsule surface, as observed in the Hawaiian bobtail squid [5, 6]. This microbiota is acquired through horizontal transmission from environmental bacterial communities [7–9], and its composition changes during female maturation [8, 10]. Thus, microbiota composition is critical for ensuring embryonic survival in some cephalopods.

The ANG is present in most Decapodiformes (excluding Oegopsidae) but is absent in Octopodiformes [11]. Most cephalopods exhibit a similar ANG structure, composed of tubules lined with epithelial cells that house extracellular bacteria [4, 7–9]. Despite the presence of distinct microbial communities in the ANGs of different cephalopod species, the microbiomes of abundant bacterial species may drive phylosymbiosis [12]. Moreover, the ANG microbiota composition is relatively stable and unaffected by environmental factors such as location and collection time for the same cephalopod species [6, 12]. In the Hawaiian bobtail squid, ANGs were either absent or underdeveloped when squid were raised in environments with low microbial exposure, highlighting the influence of early-life microbial encounters and host genetics on ANG development, rather than environmental conditions alone [13]. However, the mechanisms underlying symbiont regulation and microbiota changes in the ANG during female maturation remain unclear.

In the Hawaiian bobtail squid, *V. fischeri* produces bioluminescence in the light organ, regulated by a daily biological rhythm through quorum sensing [14, 15]. Additionally, in some cephalopods, a consortium of microbes synthesizes carotenoids that accumulate in the ANG during female maturation [4, 8, 9, 16, 17]. In cuttlefish (*Sepia officinalis*), the main carotenoid produced by ANG-isolated bacteria is the keto carotenoid, adonixanthin ($C_{40}H_{54}O_3$) [18]. Carotenoid accumulation (pigment formation) is often observed under stressful conditions as a response to harmful environments [19–21]. High bacterial density can also lead to carotenoid accumulation, regulated by quorum sensing [22]. In Hawaiian bobtail squid, the pigment indigoidine produced by ANG-isolated bacteria exhibited antimicrobial activity against several marine *Vibrio* species [23]. Therefore, pigment accumulation may not only serve as an indicator of female maturation in some cephalopods but also be an important selection factor for antimicrobials produced by ANG bacteria.

In bigfin reef squid, mature squid (with mature eggs observed in the oviduct) have a pigmented ANG (mostly white, yellow, and orange, with few red) and large numbers of bacterial community [9]. Our research aims to move beyond merely correlating microbial compositions with host genetics (e.g., different cephalopod species; [12]) and phenotypes (e.g., different ANG stages; [8, 10]). Indeed, we seek to elucidate the mechanism by which color-dependent microbes enhance reproductive fitness (final maturation) using an amplicon-based approach. We first employed 16S rRNA gene community analysis to characterize both the conserved ANG microbiome across different cephalopod species and the unique ANG microbiome in the bigfin reef squid. Subsequently, we collected different microbiota (distinguished by color differences) to identify the abundant microbiota in each pigmented region of the female bigfin reef squid. We also used qPCR analysis to study the host responses (mRNA expression of some immune-related genes) in mainly pigmented regions of ANG in mature female (spatial response). The results of this study are expected to illustrate microbial heterogeneity across different ANG regions (microbiota) within the same individual and provide valuable insights into functional interactions between bigfin reef squid and their associated microbiomes.

Methods

Field sampling

Golden cuttlefish (*Sepia esculenta*), swordtip squid (*Uroteuthis edulis*), and bigfin reef squid samples were purchased from a fisherman on Heping Island, Keelung, Taiwan. These cephalopods were collected using hand jigging from a boat off the near region of Heping Island, the northeastern coast of Taiwan. Cephalopods were

captured at night and were kept in the flowing seawater system on boat, and then were transported to the tank on next morning. After checking sex and reproductive stage, mature females were determined based on mature eggs in oviduct [24], cephalopods were transported to the laboratory at the National Taiwan Ocean University for further processing within 12 h of collection. Cephalopods were anesthetized with 5% ethanol in seawater at room temperature and then decapitated after tissue sampling. ANGs were carefully dissected using sterilized scissors. ANG from three cephalopod species were used to infer potential genetics differences in the microbiome (Fig. 1A-C). The relative size of the ANG (ANG-somatic index, ASI) differed significantly among the three species, with the golden cuttlefish having the highest ASI (Fig. 1D). Due to the distinct size of ANG in different cephalopod species, the collected ANG (left one of pair) was homogenized, centrifuged at low speed (200 × g) to remove tissue debris, and then centrifuged at high speed (10,000 × g) to collect microorganisms for total DNA extraction. In the bigfin reef squid, the ANG (right one of pair) was used to collect distinct pigmented regions. Based on the distribution of distinct colors (white, yellow, and orange) in the ventral part of the ANG, larger pigmented regions were selected for sample collection under a stereomicroscope. To prevent contamination from other regions, only the upper half of each selected region was collected. The sample collecting procedure was halted when another pigment appeared. After samples collection, the ANG was cleaned by rinsing with squid saline to remove cell debris and pigment (potential microbiota). The collected samples from different pigmented regions were then used for total DNA extraction and total RNA extraction. Collected samples were stored at -80℃. A total of 3 golden cuttlefishes, 6 swordtip squids, and 8 bigfin reef squids were collected for downstream analysis. The biological information of these cephalopods was listed in Table 1.

Genotyping

Although cephalopod species were identified by morphological characteristics, we further identified species through genetics (cytochrome oxidase c subunit I, *COI*, sequences). Total DNA was extracted using the Wizard Genomic DNA purification kit (Promega) from muscle samples according to the manufacture's protocol. The *COI* gene was amplified from DNA extracts using an invertebrate-based PCR primers [25] (Table 2). The *COI* sequence alignment was performed with the cephalopods database on NCBI to determine the genetic (species).

Nucleic acid extraction

Total DNA and total RNA extraction from ANG samples using the Trizol reagent (Thermo Fisher Scientific) according to the manufacture's protocol. Trizol reagent-homogenized nucleoprotein complexes were mixed with chloroform to separate the DNA and RNA in lower phenol-chloroform phase and upper aqueous phase, respectively. DNA and RNA were precipitated by ethanol and isopropanol, respectively. Isolated DNA and RNA were quantified using the Nanodrop 2000 spectrophotometer

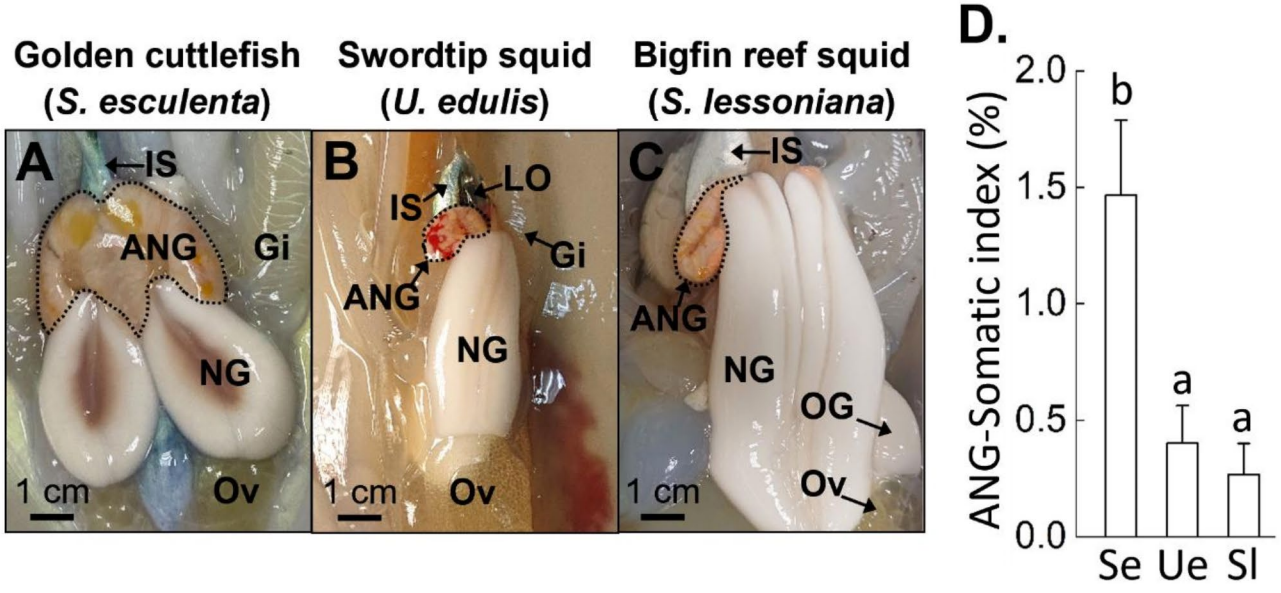

Fig. 1 Morphology and relative size of ANGs across different cephalopod species. The ANG is shown attached to the ink sac in females of the golden cuttlefish (**A**), swordtip squid (**B**), and bigfin reef squid (**C**). The relative size of the ANG is quantified as the ANG-somatic index (**D**). Lowercase letters denote significant differences as determined by one-way ANOVA followed by Tukey's multiple comparison test ($P < 0.05$). ANG, accessory nidamental gland; Gi, gill; IS, ink sac; LO, light organ; NG, nidamental gland; OG, oviductal gland; Ov, ovary, Se, golden cuttlefish; Ue, swordtip squid; Sl, bigfin reef squid

Table 1 Biological characteristics of collected cephalopods in this study

Sample name	Species (common name)	ML (cm)	BW (g)	GW (g)	ANGW (g)	GSI (%)	ASI (%)	Gonad stage
Se1	*Sepia esculenta* (Golden cuttlefish)	15	307.4	7.7	3.6	2.50	1.17	Mature
Se2		14.6	336.9	9.6	4.4	2.85	1.31	Mature
Se3		14	317.4	8.8	6.1	2.77	1.92	Mature
Ue1	*Uroteuthis edulis* (Swordtip squid)	18	141.5	4	0.4	2.83	0.28	Mature
Ue2		20	167.8	7	0.6	4.17	0.36	Mature
Ue3		20.5	203.9	9.2	0.4	4.51	0.20	Mature
Ue4		17	126.7	7.6	0.2	6.00	0.16	Mature
Ue5		19.5	147.6	9.9	0.5	6.71	0.34	Mature
Ue6		21.3	202.6	9.1	0.3	4.49	0.15	Mature
Sl1	*Sepioteuthis lessoniana* (Bigfin reef squid)	30.5	1227	4.3	0.7	0.35	0.06	Mature
Sl2		27.5	841.9	4.6	0.7	0.55	0.08	Maturing
Sl3		30	1087.6	12.8	1.3	1.18	0.12	Mature
Sl4		19.8	405.2	0.9	0.4	0.22	0.10	Maturing
Sl5		30	1154.7	20.6	1.7	1.78	0.15	Mature
Sl6		29	1167.3	18.2	1.9	1.56	0.16	Mature
Sl7		26.5	784.7	32.2	2.3	4.10	0.29	Mature
Sl8		25.9	734.8	11.9	0.9	1.62	0.12	Mature

BL, Mantle length; BW, body weight; GW, gonad weight; ANGW, accessory nidamental gland weight; GSI, gonadosomatic index; ASI, ANG-somatic index

Table 2 Oligonucleotides of primers used in this study

Gene name	Oreintation	Sequence	Analysis
CO1	Sense	5′-GGTCAACAAATCATAAAGATATTGG-3′	Genotyping
	Antisense	5′-TAAACTTCAGGGTGACCAAAAAATCA-3′	Genotyping
16S rRNA (V3-V4 region)	Sense	5′-CCTACGGGNGGCWGCAG-3′	Amplicon
	Antisense	5′-GACTACHVGGGTATCTAATCC-3′	Amplicon
EF1A	Sense	5′-CCAGGTGACAATGTTGGTTTC-3′	qPCR
	Antisense	5′-GTCTCTTTGGGTGGGTTATTCT-3′	qPCR
ACSL	Sense	5′-CGTCGGAACAGACTTGAGATT-3′	qPCR
	Antisense	5′-ATGTGTGGATGGAAAGGATAGG-3′	qPCR
UGT	Sense	5′-CGTCTCTAGCTGTTGTTGATG-3′	qPCR
	Antisense	5′-CCTGAAGGATGAAAGGAATCTG-3′	qPCR
ACL	Sense	5′-TTAGGCTGGTGTGTGTCATTAG-3′	qPCR
	Antisense	5′-CGACTCTTGTCCGCATGTAA-3′	qPCR
NOS	Sense	5′-GTTCTGGATAGACCACAGGATTT-3′	qPCR
	Antisense	5′-GTCAAGGAGGTTCGCAAGTTA-3′	qPCR
TGM1	Sense	5′-ACAGCAGCGTAACCATTGA-3′	qPCR
	Antisense	5′-GCAGGTCAGAACGAGACATATAA-3′	qPCR
PGRP2	Sense	5′-GGCACTATCTGCTGTTCAGAAT-3′	qPCR
	Antisense	5′-GCACATCCCTGTGTCCAAATA-3′	qPCR

(Thermo Fisher Scientific) and stored at -20℃ until further analysis.

PCR amplification, library preparation, and amplicon sequencing

Amplicon sequencing was performed according as described in our previous study [10]. PCR was performed using bacterial universal primers 361F and 806R (Table 2), which were designed for the bacterial V3-V4 hypervariable region of the 16S rRNA gene [26]. Thirty cycles of PCR were performed as follows: an initial step of 94℃ for 3 min, 94℃ for 15 s, 55℃ for 15 s, and 68℃ for 1 min, with 2 min at 72℃ as the final extension after the last cycle. PCR amplicons were checked by DNA agarose gel electrophoresis. PCR-amplified 350–450 bp fragments were purified using the QIAquick Gel Extraction Kit (Qiagen). DNA library construction and Illumina sequencing were conducted by Biotools, Inc. (New Taipei, Taiwan). TruSeq DNA Sample Preparation Kits (Illumina) were used for DNA library construction, and prepared libraries were quantified using a GeneRead Library Quant Kit (Qiagen). The amplicon libraries were sequenced on the Illumina MiSeq platform (Illumina) with 300 bp paired-end reads.

Amplicon analysis

Raw sequencing data (FASTQ files) were imported and analyzed using the CLC Genomic Workbench 24.0.1 (CLC Bio, QIAGEN, Aarhus, Denmark). The Illumina adapter sequences were trimmed, and the tool "QC for Sequencing Reads" was performed. "Detect Amplicon Sequence Variants (ASVs)" was used to obtain ASVs, with the first/second read lengths set as 291/268 according to the base-quality distribution from QC reports, the maximum expected errors per read set as 2.0, and detected chimeric reads were removed. Taxonomies (SILVA SSU 138.1 database) were then assigned to the ASV tables with a minimum similarity of 85%, and relative abundance tables were generated. Raising the cutoff to 90% will reduce the assigned taxonomy by approximately 12.8% (from 88.3 to 75.5%). Moreover, the proportion of uncultured/empty genus within the assigned taxonomy will increase by about 20% (from 70.3 to 50.7%). Therefore, we selected 85% and family as the level for analysis. Rarefaction curves were used retrospectively to assess sampling depth (Fig. S1). Relative abundance was calculated as the number of reads assigned to each taxon divided by the total number of quantified reads for each sample. For the data from different cephalopod species, the observed classes were applied to estimate alpha diversity, with the Shannon and Simpson indices calculated. To compute beta diversity, principal coordinate analysis (PCoA) was performed based on distance matrices generated from weighted UniFrac for ASVs and Bray-Curtis distance for bacterial classes. For the data from different ANG pigmented regions of bigfin reef squid, PCoA (Bray-Crutis distance) and alpha diversity analysis were performed for class, order, and family levels. PCoA was visualized using the R package *ggplot2* in RStudio (version 2023.12.1.402). Relative abundances of bacteria were visualized as stacked bar charts using GraphPad Prism 9.0 (GraphPad, CA, USA) and bubble plots using the R packages *ggplot2* and *reshape2*. Dot charts were created using GraphPad Prism 9.0 (GraphPad).

Table 3 ASV numbers of different cephalopod species collected in this study

Sample name	Species (common name)	ASVs	Average of ASVs
Se1	*Sepia esculenta* (Golden cuttlefish)	114	139
Se2		146	
Se3		157	
Ue1	*Uroteuthis edulis* (Swordtip squid)	130	142
Ue2		129	
Ue3		133	
Ue4		127	
Ue5		168	
Ue6		166	
Sl1	*Sepioteuthis lessoniana* (Bigfin reef squid)	229	222
Sl2		187	
Sl3		367	
Sl4		248	
Sl5		178	
Sl6		196	
Sl7		163	
Sl8		207	

ASV, amplicon sequence variant; Se, *Sepia esculenta*; Ue, *Uroteuthis edilus*; Sl, *Sepioteuthis lessoniana*

Quantitative real-time PCR

First-strand cDNA was synthesized from 1 μg qualified total RNA with Oligo(dT) 12–18 primers (Promega) using Superscript III (Thermo Fisher Scientific). The cDNA was used for RNA analysis. Quantitative real-time PCR (qPCR) analysis was performed as described in our previous study [24]. Gene transcription levels were quantified by qPCR system (CFX Connect™ Real-Time PCR Detection System; Bio-Rad Laboratories) with the SYBR Green Master Mix (Bio-Rad Laboratories). The PCR specificity was confirmed by a single melting curve in unknown samples and template-contained controls. No signal was detected by qPCR in non-template controls. The reaction efficiency of different genes was evaluated by serially diluted standards. The data were analyzed according to the $2^{-\Delta\Delta}$Ct method. *Elongation factor 1 alpha* (*EF1A*) was used as an internal control to normalize the mRNA expression levels. Specific qPCR primers for target genes and its GeneBank accession numbers are listed in Table 2.

Data analysis

The data are presented as the mean ± standard deviation (SD). The values were first tested using F-test to assess variance homogeneity. For comparisons between two groups, Student's *t*-test was conducted, with Levene's test used to determine whether equal variances could be assumed. For comparisons among multiple groups, one-way ANOVA was performed, followed by a Tukey test for post hoc analysis. A significance level of $P < 0.05$ was used to indicate statistical significance.

Results

Bacterial community composition of the ANG in three cephalopod species

A total of 2,490 ASVs were obtained from 17 ANG samples of three cephalopod species (a total of 661,964 pair reads) for analysis. Of these, 347 ASVs (13.9%) were observed in golden cuttlefish, 720 ASVs (28.9%) in swordtip squid, and 1,452 ASVs (58.3%) in bigfin reef squid (Table S1). Additionally, the average number of ASVs per sample was 139 for golden cuttlefish, 142 for swordtip squid, and 222 for bigfin reef squid (Table 3). The bigfin reef squid might have higher diversity of microbiome in the ANG compared to the other two species. When comparing species-specific ASVs (present

in over 60% samples of each species), 70 ASVs (20.2% of ASVs observed in this species) were conserved in golden cuttlefish, 15 ASVs (2.1%) in swordtip squid, and 12 ASVs (0.8%) in bigfin reef squid (Table S2). Notably, none of the ASVs were shared among the three species.

Given this lack of shared ASVs, we further analyzed the relative abundances and taxonomy at different levels. In evaluating all samples, 2,211 ASVs (88.8%) were assigned to bacterial taxa belonging to 9 phyla, 13 classes, 30 orders, and 56 families. In terms of abundance, shared classes comprised with relative proportion higher than 1% in at least one species and were present in over 60% samples for each species. Among these samples, 8 classes showed abundance in ANG (Fig. 2A and B). Of these, samples from golden cuttlefish largely consisted of *Alphaproteobacteria* (62.4%) and *Bacteroidia* (34.6%). In swordtip squid, the bacterial community was dominated by *Alphaproteobacteria* (47.2%), *Gammaproteobacteria* (36.6%), *Bacteroidia* (10.9%), and to a lesser extent, *Acidimicrobiia* (5.3%). In bigfin reef squid, the community was dominated by *Bacteroidia* (42.6%), *Alphaproteobacteria* (27.3%), *Gammaproteobacteria* (19.4%), with lesser contributions from *Holophagae* (7.2%) and *Verrucomicrobiae* (2.7%). Altogether, *Alphaproteobacteria* and *Bacteroidia* were shared in all ANG samples, while *Gammaproteobacteria* were greatly shared in swordtip squid and bigfin reef squid. Moreover, *Acidimicrobiia* was exclusively associated with swordtip squid, while *Holophagae* and *Verrucomicrobiae* were mainly associated with bigfin reef squid. These findings revealed that bacterial composition of ANG at class levels may vary depending on the cephalopod species.

Principal coordinates analysis (PCoA) revealed that the microbial community structure (beta diversity) of ANGs clustered distinctly by species (Fig. 2C and D). This was further confirmed by PERMANOVA of beta diversity metric using weighted UniFrac (ASV level, pseido-$F = 11.235$, p-value < 0.001) and Bray-Curtis

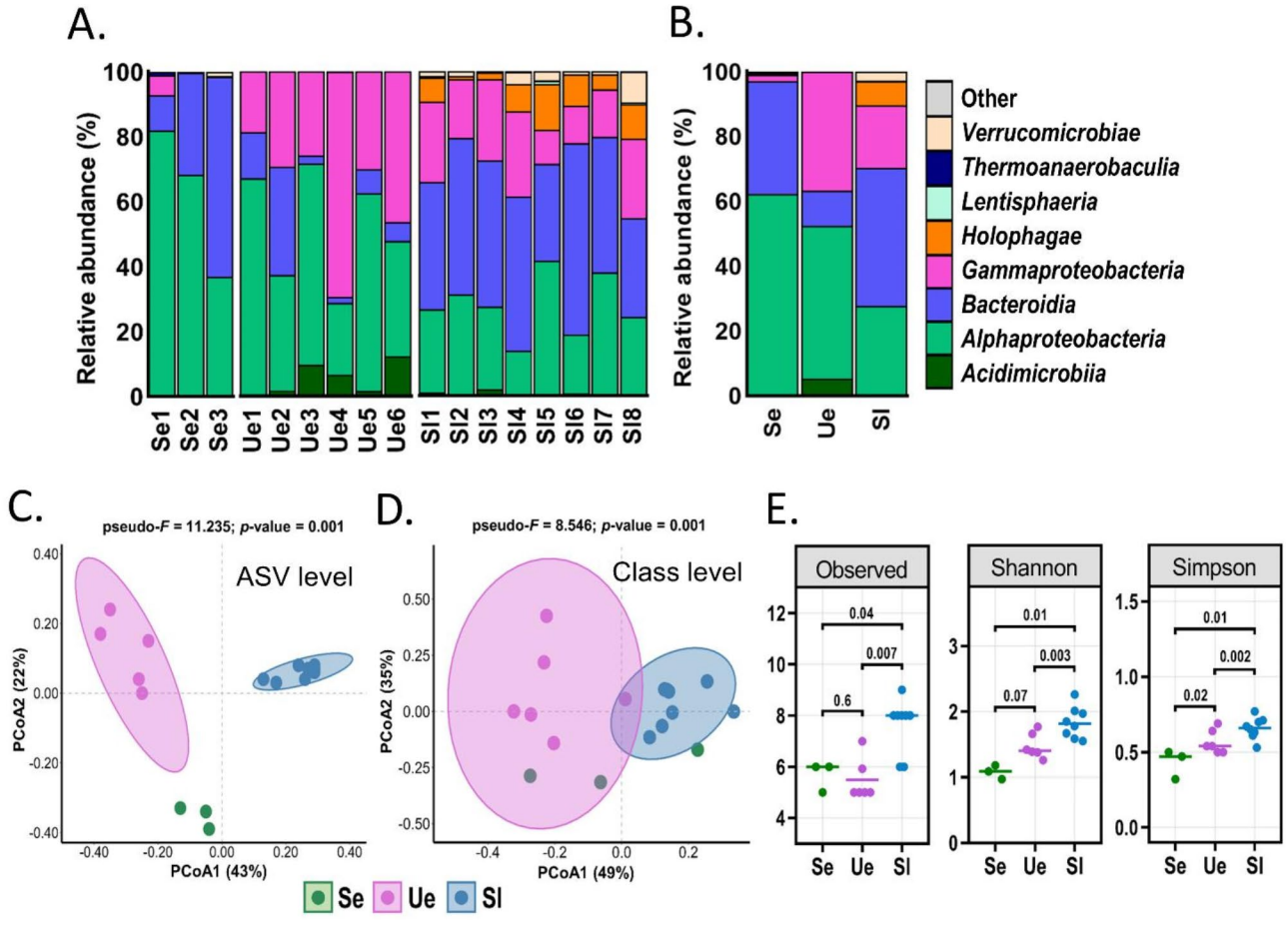

Fig. 2 Microbiomes and bacterial diversity of ANGs across different cephalopod species. Bacterial community composition (**A**) and the mean relative abundance (**B**) of bacterial classes associated with ANGs in golden cuttlefish, swordtip squid, and bigfin reef squid. Bacterial classes with global relative abundances of < 1% are grouped as "Other". Principal coordinate analysis (beta diversity) of bacterial ASVs (**C**) and classes (**D**) across different cephalopod species as assessed by weighted UniFrac using Bray-Curtis distance. Alpha diversity (**E**) indices of bacterial class between different cephalopod species. Observed indices of richness and Shannon's and Simpson's indices of diversity. Se, golden cuttlefish; Ue, swordtip squid; Sl, bigfin reef squid

distance (class level, pseudo-$F = 8.546$, p-value < 0.001). Broadly, alpha diversity analysis showed significant differences between the bigfin reef squid, golden cuttlefish and swordtip squid (Fig. 2E), although no significant differences in bacterial richness or evenness (Observed and Shannon indices) were observed between the golden cuttlefish and swordtip squid (Fig. 2E). Altogether, these results indicate that the bigfin reef squid exhibited the highest richness and evenness in the ANG microbiome, while the golden cuttlefish and swordtip squid had lower diversity.

The characteristics of the ANG in mature female of bigfin reef squid

Based on the size of pigmented regions, numerous small pigmented regions were observed in the dorsal part of the ANG (Fig. 3A). In contrast, several large pigmented regions were noted in the ventral part of ANG, adjacent to the ink sac (Fig. 3B). Histological analysis of sagittal ANG sections revealed two distinct layers: an outer epithelial cell layer composed of primary tubules and an inner epithelial cell layer composed of secondary tubules (Fig. 3C). Regarding the epithelial cell types in the secondary tubules, sections showed that secondary tubules with similar epithelial cell types were commonly found across a broad region of the ventral part of the ANG, likely originating from the same microbiota (Fig. 3C and D). Histological analysis of a transverse section of the ANG demonstrated secondary tubules with different epithelial cell types were randomly distributed in the dorsal part of ANG, possibly housing various microbiota (Fig. 3E). Furthermore, the transverse section confirmed that secondary tubules with identical epithelial cell types were present in a wide region of the ventral part of the

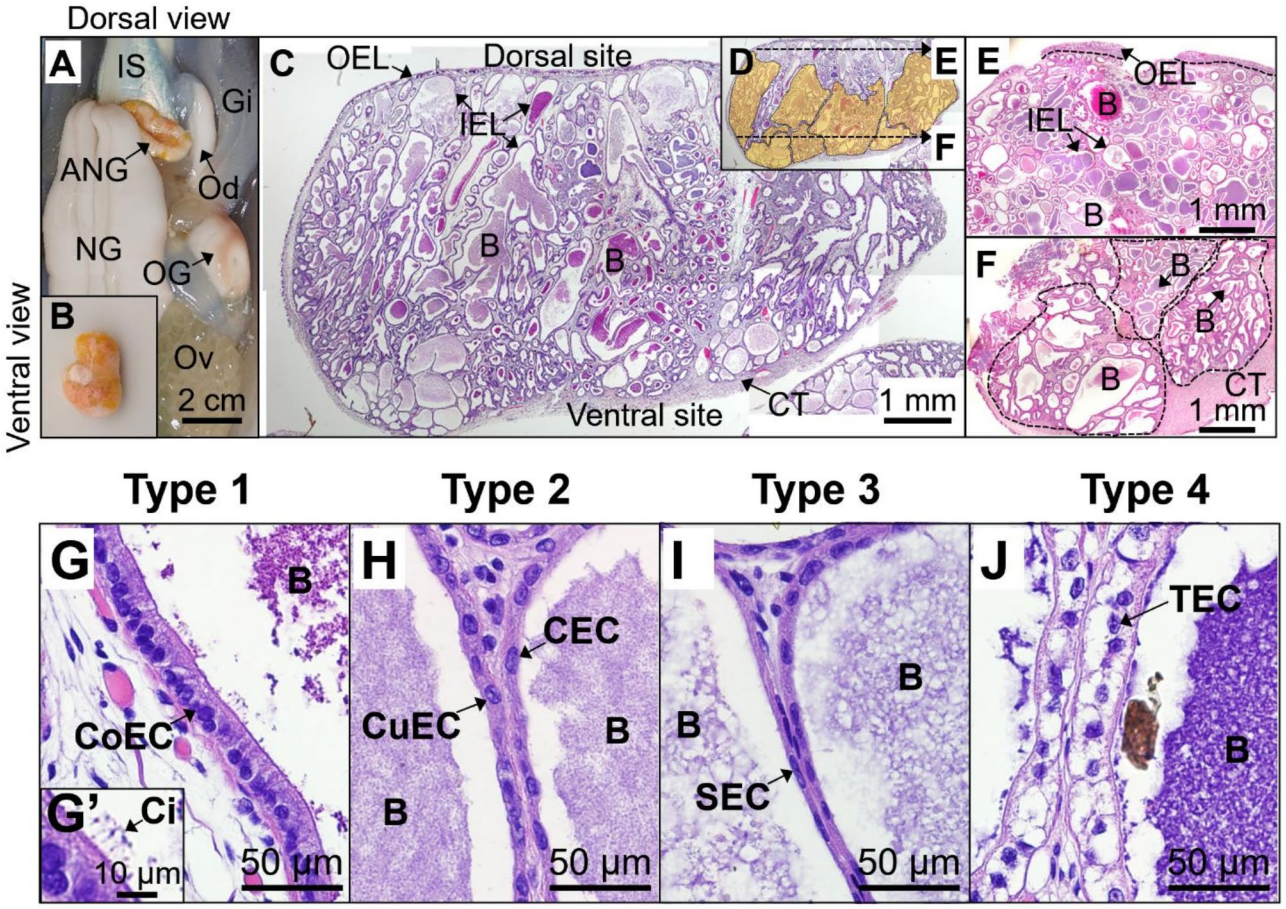

Fig. 3 Histological characteristics and bacterial distributions in the ANG of female bigfin reef squid. Dorsal (**A**) and ventral (**B**) views of the ANG in an adult female. Sagittal dissection of the ANG (**C**) and bacterial distribution (**D**). Tubular size and microbiota distribution in the dorsal (**E**) and ventral (**F**) regions. The arrows in the dorsal region (**D**) indicate the direction of the plan shown in the ventral regions (**E** and **F**). The distinct regions (yellow color) are characterized by morphology of epithelial cells and the staining color of the microbiota. Types of epithelial cells observed in secondary tubules include columnar epithelial cells (type 1; **G** and **G'**), cuboidal epithelial cells (type 2; **H**), squamous epithelial cells (type 3; 3 **I**), and transparent epithelial cells (type 4; **J**). The dash line denotes separate layers or regions based on their morphological differences. ANG, accessory nidamental gland; B, bacteria; Ci, cilia; CoEC, columnar epithelial cells; CuEC, cuboidal epithelial cells; Gi, gill; IEL, inner epithelial layer; IS, ink sac; NG, nidamental gland; Od, oviduct; OEL; outer epithelial layer; OG, oviductal gland; Ov, ovary; SEC, squamous epithelial cells; TEC, transparent epithelial cells

ANG (Fig. 3F). Therefore, these findings indicate that each cluster of secondary tubules can be distinguished by color.

Additionally, four types of epithelial cells were observed in the secondary tubules of inner ANG layer: columnar epithelial cells (type 1; Fig. 3G and G'), cuboidal epithelial cells (type 2; Fig. 3H), squamous epithelial cells (type 3; Fig. 3I), and transparent epithelial cells (type 4; Fig. 3J). Transparent epithelial cells (type 4) were rarely observed (< 1% of total area of ANG), while columnar (type 1), cuboidal (type 2), and squamous (type 3) epithelial cells were more prevalent.

Bacterial community composition in pigmented regions of ANG of bigfin reef squid

Pigmented regions of ANG (right one of pair) from six bigfin reef squid (Sl1, 3, 5–8) were further used to infer potential selection for reproduction in the ANG microbiome compared to the whole ANG (left one of pair) of each individual, including Sl1 (left ANG and 5 pigmented regions from right ANG), Sl3 (left ANG and 5 pigmented regions from right ANG), Sl5 (left ANG and 4 pigmented regions from right ANG), Sl6 (left ANG and 6 pigmented regions from right ANG), Sl7 (left ANG and 7 pigmented regions from right ANG) and Sl8 (left ANG and 4 pigmented regions from right ANG) (Fig. 4A-F). A total of 350, 426, 251, 306, 273, and 408 ASVs were obtained from 6 individuals for analysis, respectively (Table 4). Of these, the average number of ASVs per ANG sample was 223 ASVs and per pigmented region sample was 127 ASVs. The pigmented region of the ANG might have lower diversity of microbiome compared to the whole ANG tissue.

First, when comparing ASVs from the pigmentated region (present in over 60% samples of each pigmented color), 24 ASVs were conserved in the orange-pigmented regions, 17 in the white-pigmented regions, and 3 in the yellow pigmented regions. Notably, none of these ASVs were identified as core ASVs, as their relative abundance was low (present in less than 1% of over 40% of the samples) within each pigmented region. We further analyzed the relative abundances and taxonomy at different levels. ASVs represented bacterial taxa belonging to 9 phyla, 13 classes, 27 orders, and 52 families (Table S3). In terms of abundance, shared classes comprised with relative proportion higher than 1% in at least one class and present in over 60% samples. Unlike whole ANG tissue, which was composed of several classes, including *Bacteroidia* (43.7%), *Alphaproteobacteria* (26.9%), *Gammaproteobacteria* (16.8%), *Holophagae* (8.2%) and *Verrucomicrobiae* (3.9%), pigmented regions largely consisted of *Bacteroidia* (45%) and *Alphaproteobacteria* (44.6%), with a lesser extent *Holophagae* (6.6%; Fig. 4G and H). *Gammaproteobacteria* were less associated with pigmented region samples, accounting for ~ 3% and were not consistently present, being found in less than 60% of the samples (Fig. 4G and H). Thus, our data suggests that the bacterial composition was selected in pigmented region (large microbiota), with an increased abundance of *Alphaproteobacteria* potentially playing a primary role in this association.

PCoA revealed that the microbial community structure (beta diversity) of pigmented regions clustered distinctly between the orange regions and whole ANG tissues (Fig. 4I). This was further confirmed by PERMANOVA of beta diversity metric using Bray-Curtis distance (pseudo-$F = 3.455$, p-value = 0.0074) and pairwise comparison ($R^2 = 0.258$, $p = 0.0414$). Alpha diversity analysis showed significant differences between the whole ANGs and each pigmented region (Fig. 4J), although no significant differences were observed between different pigmented regions (Fig. 4J). Furthermore, at different levels (from ASV to family), PCoA results showed significant differences between the whole ANGs and pigmented regions, particularly at the family level where differences were observed between almost all groups according to the pairwise comparison (Fig. S2). These analyses suggest that distinct microbial compositions were prominently observed at the family level, providing a suitable basis for further analysis.

Color-associated bacteria in ANG of the bigfin reef squid

To understand the relationship between pigmented regions (microbiota color) and bacterial communities, we further analyzed the relative abundances and taxonomy at the family level. In terms of abundance, shared families comprised with relative proportion higher than 1% in at least one sample and present in over 60% samples for each color. Among the identified bacterial families (Fig. 5A), five were conserved in at least one pigmented region (present in > 60% samples of a given pigmented region). Three families were represented in the orange pigmented region, four families were represented in the white pigmented region, and two families were represented in the yellow pigmented region (Fig. 5A). Samples from orange pigmented regions largely consisted of *Hyphomicrobiaceae* (40.4%) and *Cryomorphaceae* (27.6%), and to a lesser extent, *Rhodobacteraceae* (10.9%) and *Flavobacteriaceae* (8.1%; Fig. 5B). White pigmented regions largely consisted of *Cryomorphaceae* (34.2%) and *Fodinicurvataceae* (24.7%), with smaller proportions of *Rhodobacteraceae* (17.5%) and *Flavobacteriaceae* (11.5%) (Fig. 5B). Yellow pigmented regions largely consisted of *Cryomorphaceae* (45.5%) and *Rhodobacteraceae* (10.6%) (Fig. 5B). Altogether, *Rhodobacteraceae*, *Cryomorphaceae* and *Flavobacteriaceae* were abundantly shared among the three colors of microbiota. *Hyphomicrobiaceae* were unique to orange microbiota, *Fodinicurvataceae* were

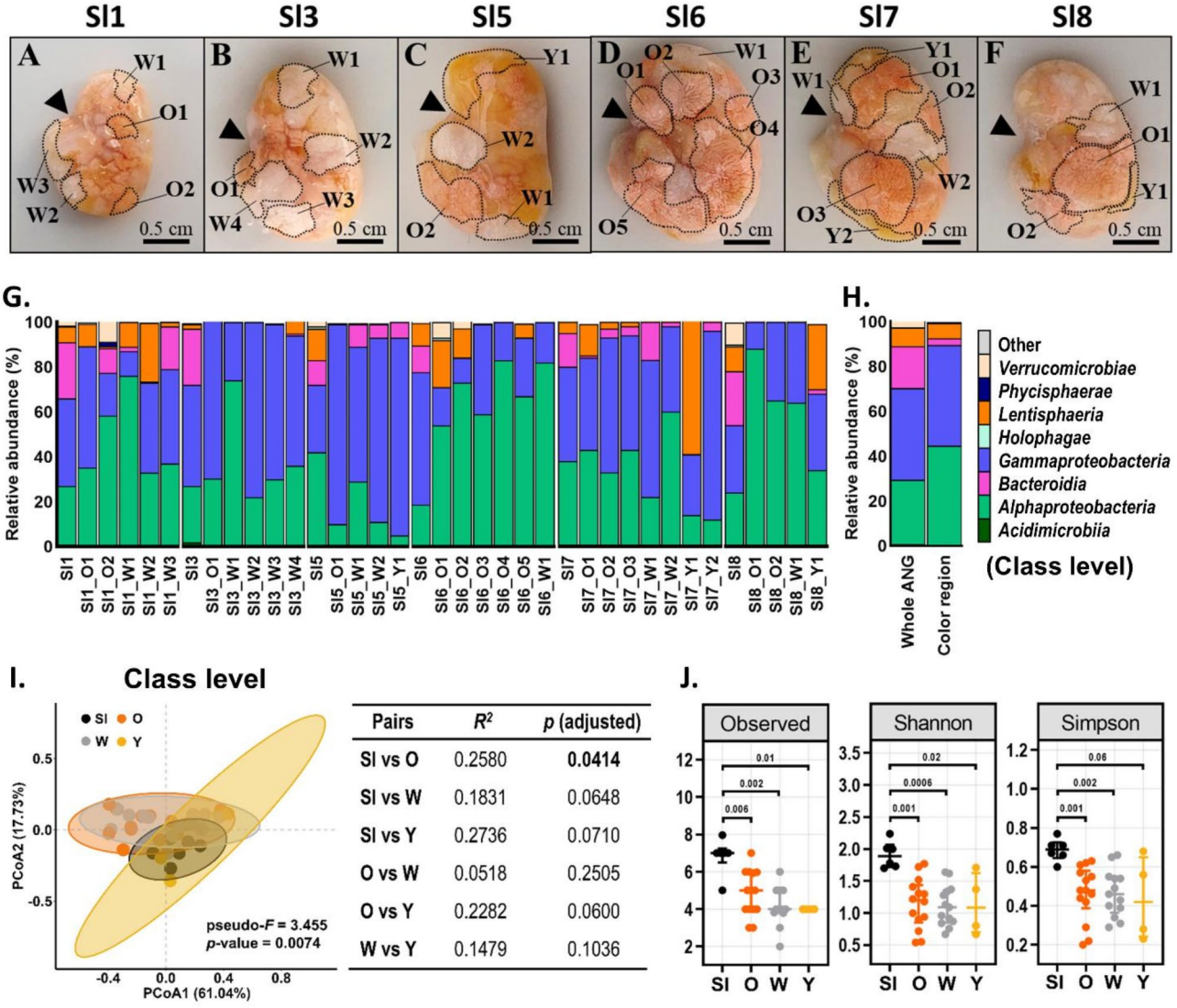

Fig. 4 Microbiomes and bacterial diversity of ANGs and their associated microbiota across different individuals. Microbiota distribution on the right side of the ANG collected from different individuals (**A**-**F**), with specific pigmented regions highlighted. Bacterial community composition (**G**) and mean relative abundance (**H**) of bacterial classes associated with whole ANGs (left side of ANG pair) and pigmented regions (right side of ANG pair) from different individuals. Bacterial classes with < 1% global relative abundances are presented as "Other". Principal coordinate analysis (beta diversity) of bacterial classes (**I**) across whole ANGs and their associated pigmented regions, assessed by weighted UniFrac (ASV level) and Bray-Curtis distance (class level). The results of principal coordinate analysis of bacterial order and family are shown in Figure S2. Alpha diversity (**J**) indices of bacterial classes between whole ANGs and isolated pigmented regions. Observed indices of richness and Shannon's and Simpson's indices of diversity. O, orange; SI, bigfin reef squid; W, white; Y, yellow

unique to white microbiota, and *Acanthopleuribacteraceae* were unique to yellow microbiota. The families with an average relative abundance greater than 1% in at least one pigmented group were shown in Fig. 5C. Our results showed significant differences in *Fodinicurvataceae*, *Hyphomicrobiaceae* and *Acanthopleuribacteraceae*. Some differences could still be observed in *Crocinitomicaceae*, *Cellvibrionaceae* and *Rubritaleaceae*, although they were not statistically significant.

Gene expression profiles in different pigmented regions of bigfin reef squid

The immune response is the dominant KEGG pathway in the early transmission and middle colonization phases, while lipid metabolism and the metabolism of bacterial flora fermentation are the dominant KEGG pathways in the late pigmentation phase [34]. Some of these differentially expressed genes associated with female maturation were selected for analysis by qPCR, including lipid metabolic process-associated genes (*acyl-CoA synthetase long chain family*, *ACSL*; *UDP-glucuronosyltransferase*, *UGT*;

Table 4 ASV numbers of whole ANG and pigmented region samples of Bigfin reef squid

Sample name	Type	ASVs	Average of ASVs
SI1	Whole ANG (left one of pair)	229	223
SI3		367	
SI5		178	
SI6		196	
SI7		163	
SI8		207	
SI1_O1	Pigmented region (right one of pair)	195	127
SI1_O2		165	
SI1_W1		109	
SI1_W2		149	
SI1_W3		221	
SI3_O1		142	
SI3_W1		87	
SI3_W2		155	
SI3_W3		122	
SI3_W4		116	
SI5_O1		136	
SI5_W1		98	
SI5_W2		139	
SI5_Y1		130	
SI6_O1		139	
SI6_O2		84	
SI6_O3		99	
SI6_O4		94	
SI6_O5		104	
SI6_W1		97	
SI7_O1		53	
SI7_O2		127	
SI7_O3		129	
SI7_W1		197	
SI7_W2		143	
SI7_Y1		124	
SI7_Y2		100	
SI8_O1		103	
SI8_O2		127	
SI8_W1		127	
SI8_Y1		112	

ASV, amplicon sequence variant; ANG, accessory nidamental gland; O, orange; W, white; Y, yellow

acid ceramidase-like, *ACL*) and immune response-associated genes (*nitric oxide synthase*, *NOS*; *transglutaminase 1*, *TGM1*; *peptidoglycan recognition protein 2*, *PGRP2*) (Fig. 6). qPCR results revealed that lipid metabolic process-associated genes (*ACSL*, *UGT*, and *ACL*) had similar transcription levels between the different pigmented regions. In contrast, despite the *PGRP2*, other immune response-associated genes (*NOS* and *TGM1*) showed higher transcription levels in orange region than in other regions (yellow and white).

Discussion

While the host-microbiota communication within the light organ of the bobtail squid is well studied, the interaction within the accessory nidamental gland (ANG) of cephalopods remains poorly understood. The bigfin reef squid, *Sepioteuthis lessoniana*, serves as an excellent model for ANG research due to its larger ANG size compared to the bobtail squid. In this study, we aimed to investigate the composition of the pigmented region-associated microbiome using an amplicon-based approach. Based on our literature review, this is the first 16 S bacterial community study of the ANG to examine spatial variations across different pigmented regions in cephalopods. We observed three main types of epithelial cells in the secondary tubules of the ANG (Fig. 3), which were consistently present in the same tubules and adjacent regions. Using this characteristic, we collected ANG samples based on their pigmented and performed amplicon-based analyses (Fig. 4). When comparing the microbiome of whole ANG tissues to that of specific pigmented regions, we found that microbial richness and diversity were significantly reduced in the pigmented regions. Notably, the abundance of *Alphaproteobacteria* was significantly higher in these regions compared to the whole ANG. Furthermore, in mature females, we identified two distinct microbiomes corresponding to different pigmented groups: orange and non-orange (yellow and white) regions (Fig. 5). Several pigmented region-associated bacteria were observed in bigfin reef squid, suggesting a correlation between bacterial composition and tissue pigmentation. Collectively, our findings provide valuable insights into the interactions between bigfin reef squid and its associated microbiomes, highlighting potential roles of specific bacterial communities in different pigmented regions of the ANG.

Species-specific and Reproductive-associated microbiome in the ANG of bigfin reef squid

High abundances of *Alphaproteobacteria* were detected in all cephalopod species analyzed in this study, including the gold cuttlefish, swordtip squid, and bigfin reef squid, as reported in a previous study [12]. Compared to the Japan-collected bigfin reef squid in previously study [12], our data showed the higher abundances of *Bacteroidia* (with *Flavobacteriia*) and *Gammaproteobacteria* in Taiwan-collected samples. Beta diversity analyses revealed significant microbiome differences between species, while alpha diversity varied significantly among cephalopod species but showed no correlation to their taxonomic families (Fig. 2). Notably, the bigfin reef squid exhibited a richer bacterial community compared to the golden cuttlefish and swordtip squid, with no significant difference observed between the golden cuttlefish and swordtip squid. Despite the high abundances of

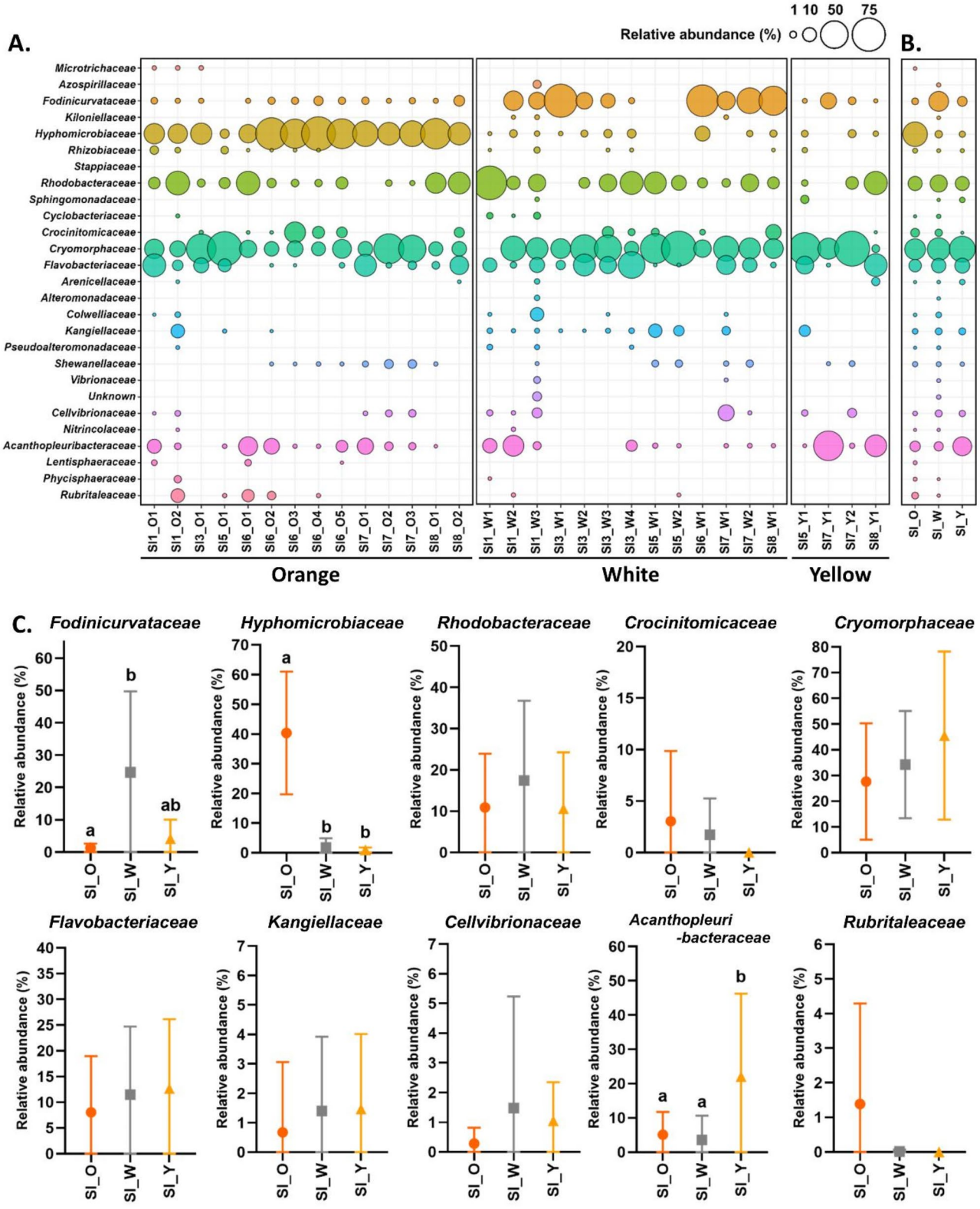

Fig. 5 Pigmented-associated bacterial families in ANGs. Bacterial community composition (**A**) and mean relative abundance (**B**) of bacterial families associated with pigmented regions from individuals. Bacterial families with global relative abundances of < 1% are grouped as "Other". Circle size represents the relative abundance (%) of each bacterial family. Shared bacterial families, defined as those present in > 60% of samples within a given pigmented region, are compared to show the differences among pigmented regions (**C**). Lowercase letters denote significant differences as determined by one-way ANOVA followed by Tukey's multiple comparison test ($P < 0.05$). O, orange; SI, bigfin reef squid; W, white; Y, yellow

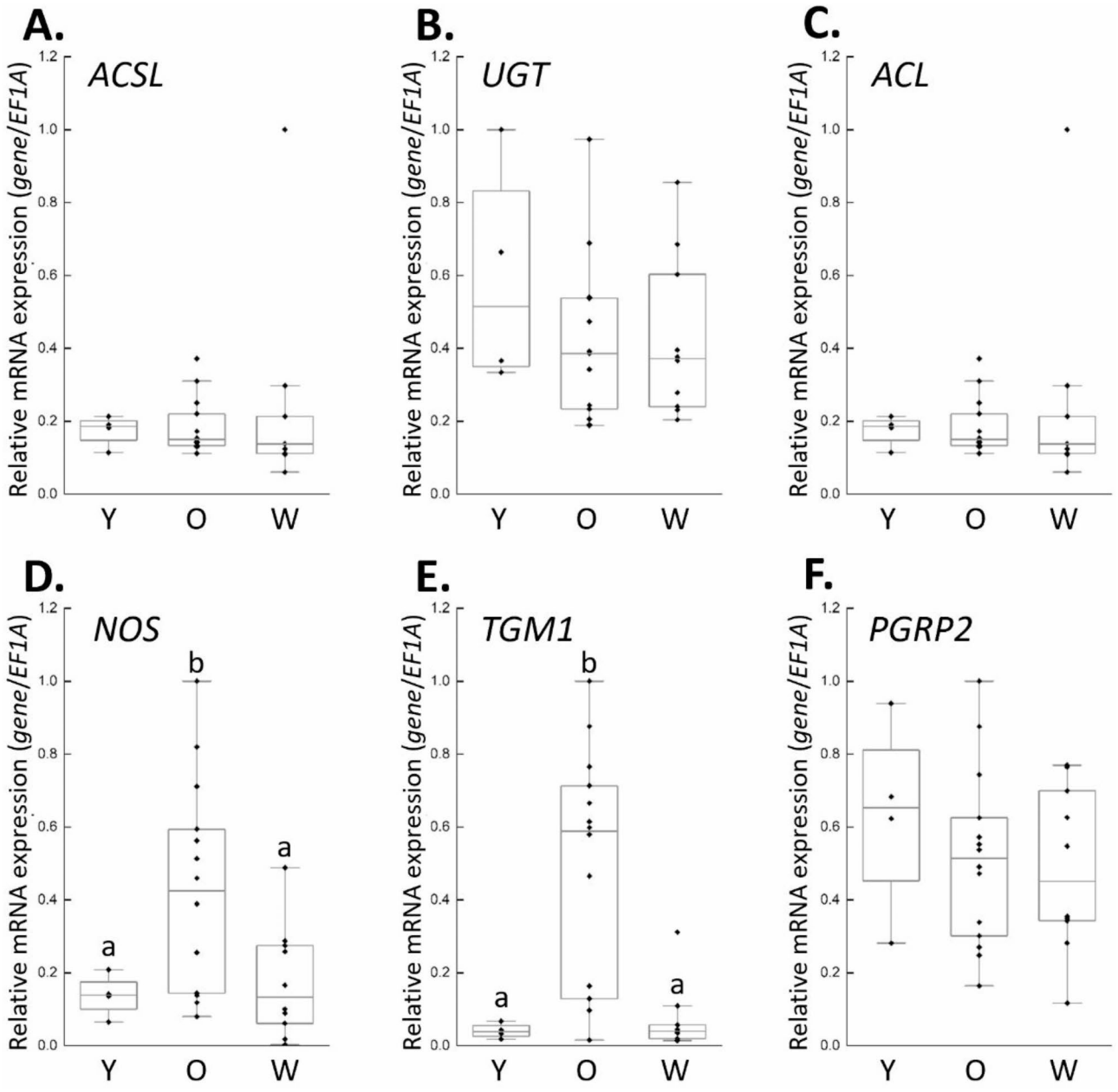

Fig. 6 Genes expression profiles in pigmented regions of the ANG. Expression profiles of selected host genes were analyzed by qPCR, including lipid metabolic process-associated genes: *acyl-CoA synthetase long chain family*, *ACSL* (**A**); *UDP-glucuronosyltransferase*, *UGT* (**B**); *acid ceramidase-like*, *ACL* (**C**), and immune response-associated genes: *nitric oxide synthase*, *NOS* (**D**); *transglutaminase 1*, *TGM1* (**E**); *peptidoglycan recognition protein 2*, *PGRP2* (**F**). Differences between pigmented regions were normalized to *Ef1a* gene expression, with the highest relative value of gene transcript level set to 1. Lowercase letters denote significant differences as determined by one-way ANOVA followed by Tukey's multiple comparison test ($P < 0.05$). O, orange; W, white; Y, yellow

Bacteroidia in Taiwan-collected bigfin reef squid (this study), we also observed substantial variability in *Bacteroidia populations* both within and across cephalopod species [12]. These findings suggest that *Alphaproteobacteria* may play a crucial role in cephalopod symbiosis, while the abundance of *Bacteroidia* might be linked to differences in habitat microbiomes.

When comparing the whole ANG tissues to distinct pigmented regions, we observed a lower diversity of microbiomes in the pigmented regions, with a shift in bacterial composition from low *Alphaproteobacteria* and high *Gammaproteobacteria* to high *Alphaproteobacteria* and low *Gammaproteobacteria*. In the Hawaiian bobtail squid, *Alphaproteobacteria* abundance positively correlates with squid size, which is itself positively correlated with reproductive stage [8]. This suggests that *Alphaproteobacteria* may play a significant role in the ANG

symbiosis of bigfin reef squid, particularly in relation to reproductive fitness.

In mature female bigfin reef squid, *Cryomorphaceae* (a clade of *Bacteroidia*) and *Rhodobacteraceae* (a clade of *Alphaproteobacteria*) were common across the three pigmenteds regions, while *Hyphomicrobiaceae* (a clade of *Alphaproteobacteria*) was unique to the orange microbiota. Additionally, *Fodinicurvataceae* (a clade of *Alphaproteobacteria*) and *Flavobacteriaceae* (a clade of *Bacteroidia*) were unique to the white microbiota (Fig. 5). These shared bacterial taxa showed significant differences in abundances between the pigmented regions, demonstrating a strong correlation between specific bacterial communities and microbiota pigmentation. Pigmentation is a key morphological characteristic of the ANG during female maturation, with the ANG changing color from white to yellow and orange as female bigfin reef squid undergo sexual maturation. In bigfin reef squid, color of the ANG changes from white to yellow and orange during sexual maturation [9, 16]. These ANG-associated bacteria, particularly *Alphaproteobacteria* and *Bacteroidia* (including *Flavobacteriia*), are vital for embryonic survival, as they prevent fungal fouling on egg capsule surface, as previously observed in the Hawaiian bobtail squid [5, 6]. Altogether, our findings suggest that *Hyphomicrobiaceae* (*Alphaproteobacteria*) may be selected by the host and play a critical role in enhancing reproductive fitness in the bigfin reef squid.

ANG pigmentation caused by accumulation of microbially-synthesized carotenoids

In this study, our data reveal that the richness and diversity of the microbiome were significantly decreased with increased abundance of *Alphaproteobacteria* in the pigmented regions compared to the whole ANG (Figs. 4 and 5). Additionally, our data also reveal that the microbiome of different ANG regions are associated with the microbiota color of regions (Fig. 5). The color of the ANG changes from white to yellow and orange during sexual maturation in female bigfin reef squids [9, 16]. These colors are due to the accumulation of carotenoids in the ANG tubules, synthesized by commensal microbes in female squid [17]. Carotenoid synthesis occurs in some bacterial species under stressful environmental conditions such as variable light, salinity, and temperature (reviewed in [27]). Furthermore, carotenoid synthesis is regulated by high bacterial density through the quorum-sensing system in certain bacteria [22]. Thus, pigmentation may be due to different stress conditions [19–21], but antimicrobial production can also be linked to pigment production and thus may be part of the symbiotic function in the ANG. Altogether, the association of microbes with a given color may be causal.

Several members of marine *Flavobacteriales* (clade of *Bacteroidia*), including *Flavobacteriaceae* and *Cryomorphaceae*, are known to produce carotenoids, Flexirubin-type pigments, or both [20, 28, 29]. In Hawaiian bobtail squid, pigmentation change in ANG has previously been attributed to *Alphaproteobacteria*, particularly members of the *Rhodobacteraceae* family [30]. Additionally, based on the present data in our studies (this study; [10]), we suggest that both *Bacteroidia* and *Alphaproteobacteria* contribute to the pigmentation observed in the mature ANG of bigfin reef squid. *Flavobacteriales* through their production of carotenoids and Flexirubin-type pigments, likely play a crucial role alongside *Alphaproteobacteria* in shaping the distinct coloration of the ANG during cephalopod maturation.

The phenotypes of epithelial cells-formed barrier may be shaped by microbiota

The ANG tubules of bigfin reef squid have a multi-branched, blind-end structure lined with a single layer of epithelial cells that house microbiota [9]. In this study, three main types of epithelial cells were observed in the ANG tubules: columnar epithelial cells, cuboidal epithelial cells, and squamous epithelial cells (Fig. 3). The host typically provides both physical and chemical barriers to segregate symbiotic microorganisms. The physical barrier consists of epithelial cells and associated immune cells tailored for each location. However, epithelial function can be modulated by microbes (reviewed in [31]). For instance, in the mammalian intestine, gut microbiota converts dietary fiber into fermentation products like short-chain fatty acids, which promote barrier function [32]. In lung diseases such as asthma, perturbations of barriers associated with compositional changes to microbial communities are loosely linked [33]. Therefore, microbial communities are often associated with a given phenotype.

In cephalopods, ANG tubules are densely colonized with a variety of microbes, and the bacterial compositions shift during female maturation [8, 10]. The microbiota of the ANG is not affected by environmental conditions, location, or collection time of the same cephalopod species [6, 12]. Moreover, ANGs were either absent or poorly developed when Hawaiian bobtail squid were raised without habitat-associated bacteria [13]. Therefore, our data suggest that different epithelial cell types of ANG tubules may be associated with the compositions of microbiota.

Potential host-selected regulatory mechanisms during pigmentation in cephalopod

Our recent study showed that the immune response is the dominant KEGG pathway in the early transmission and middle colonization phase, while lipid metabolism

and the metabolism of bacterial floral fermentation are the dominant KEGG pathways in the late pigmentation phase [34]. In the present study, some differentially expressed genes associated with female maturation were selected for analysis by qPCR, including metabolic process-associated (*ACSL*, *UGT*, and *ACL*) and immune-associated genes (*NOS*, *TGM1*, and *PGRP2*). Although most of selected genes showed that transcript levels are not associated with the pigmented regions of ANG, but some immune-related genes (*NOS* and *TGM1*) showed strong correlation with the color of region and higher transcription levels in orange region (Fig. 6).

In mammalian intestine, anaerobic bacteria produce metabolites such as butyrate, acetate, and propionate, which help adjust epithelial metabolism and homeostasis [35, 36]. Similarly, bi-directional metabolic interactions between hosts and microbes have been found in animals, involving nutrient allocation and substrate transfer [37, 38]. Therefore, our data suggest that the metabolic states of epithelial cells in the ANG may not only contribute to maintaining ANG homeostasis but also regulating the composition of the commensal microbs at a global level (ANG stage) rather than at the local level (pigmented region) in bigfin reef squid.

Host immunity plays a significant role in regulating host-microbiota interactions. The innate immune responses have been studied in several cephalopod species [39]. Although our recent data indicate a reduction in transcriptomic levels of most immune-related genes in ANGs during female maturation-such as pattern recognition receptors, cytokines, and immune-mediated transcription factor [34]. Our recent study also shows that the transcription of some immune-related genes, such as *PGRP2*, alkaline phosphatase (*ALP*), and *CD109*, significantly increase during female maturation in the bigfin reef squid [16, 34]. Furthermore, bigfin reef squid *PGRP2* and *CD109* are mainly expressed in the epithelial cells of certain ANG tubules (present study; [16]). In Hawaiian bobtail squid, secreted PGRP2 play an integral role in recognizing symbiotic bacteria during the colonization of the crypts of the light organ by *Vibrio fischeri* [40]. PGRP2 exhibits bactericidal activity in both the bigfin reef squid [16] and Hawaiian bobtail squid [40]. Therefore, our data suggest that the expression of immune-related genes in certain ANG regions may help maintain the density or composition of the total commensal microbes in mature squid.

Conclusions

The bigfin reef squid is a valuable commercial cephalopod species in East Asia, though its farming has yet to reach a commercial scale. Key challenges include issues such as cannibalism, feed supply, and particularly low hatching rates in breeding programs. In some squid species, parent-delivered microbes play a crucial role in preventing lethal biofouling on eggs and enhancing offspring hatching rates. Thus, understanding the regulatory mechanisms behind host-microbiota interactions is essential for improving aquaculture success.

In this study, we identified two distinct microbiome groups within specific regions of the ANG, distinguished by their microbiota colors. We found that certain bacterial families are closely associated with specific pigmented regions, identifying both orange region-dependent and orange region-independent bacteria. Building on this discovery, we propose developing in situ hybridization techniques to detect host-expressed genes and study the local communication between the epithelial cell types of secondary tubules. Using pigmented region-associated bacteria as markers, this approach will enable us to investigate gene expression profiles within different ANG pigmented regions. This advancement provides a pathway to better understand the regulatory mechanisms of host-microbiota interactions at tissue-specific and region-specific levels in the bigfin reef squid.

Supplementary Information

The online version contains supplementary material available at https://doi.org/10.1186/s42523-025-00402-2.

Supplementary Material 1: **Supplemental Fig. 1**: Rarefaction curves from the ANG samples of different cephalopod species and isolated pigmented regions of Bigfin reef squid. The ASV richness of ANG microbiota across cephalopod species (A) and isolated pigmented regions of bigfin reef squid (B) is displayed using rarefaction curves. A flatter curve indicates sufficient sequencing depth, having reached saturation. The X-axis represents the number of reads per sample, and the Y-axis shows ASV richness. O, orange; Se, golden cuttlefish; Sl, bigfin reef squid; Ue, swordtip squid; W, white; Y, yellow.

Supplementary Material 2: **Supplemental Fig. 2**: Bacterial diversity of ANGs and their associated microbiota across different individuals at different levels. Principal coordinate analysis (beta diversity) of bacterial ASV (A), order (C) and family (E) across whole ANGs and it associated pigmented regions as assessed by weighted UniFrac using Bray-Curtis distance. The results of principal coordinate analysis of bacterial class are shown in Fig. 4I. Alpha diversity indices of bacterial ASV (B), order (D) and family (F) between whole ANGs and isolated pigmented regions. Observed indices of richness and Shannon's and Simpson's indices of diversity. O, orange; Sl, bigfin reef squid; W, white; Y, yellow.

Supplementary Material 3

Supplementary Material 4

Supplementary Material 5

Acknowledgements

We thank Mr. Cyuan-Hong Syu and Mr. Yao-Jen Tsou for their assisting in collecting squids in Keelung. We thank Dr. Peng-Wei Tseng and Ms. Ying-Syuan Lyu at National Taiwan Ocean University for assisting of the manuscript.

Author contributions

LC analyzed the amplicon data, created the figures, and wrote the draft manuscript. JLG performed sample collection, DNA extraction, genetic identification of cephalopods, and initial amplicon analysis. HWL was involved in sample collection and RNA analysis. HJC conducted the preliminary analysis of the amplicon data. SHY supervised the amplicon analysis and contributed

to editing and review the manuscript. SD edited and reviewed the manuscript. CFC provided resource support and participated in editing and reviewing the manuscript. YCT supervised the investigation and participated in editing and reviewing the manuscript. GCW was responsible for conceptualization, supervision, funding acquisition, and was a major contributor to writing the manuscript. All authors read and approved the final manuscript.

Funding
This work was partly supported by grants from the National Science and Technology Council [NSTC 111-2326-B-019-001-MY3] and by the Center of Excellence for the Oceans, National Taiwan Ocean University, from The Featured Areas Research Center Program within the framework of the Higher Education Sprout Project by the Ministry of Education (MOE) of Taiwan.

Data availability
The raw sequence data has been uploaded to NCBI Sequence Read Archive database under BioProject ID PRJNA1182936.

Declarations

Competing interests
The authors declare no competing interests.

Author details
[1]Institute of Oceanography, National Taiwan University, Taipei, Taiwan
[2]Marine Research Station, Institute of Cellular and Organismic Biology, Academia Sinica, Yilan, Taiwan
[3]Department of Aquaculture, National Taiwan Ocean University, Keelung, Taiwan
[4]Institute of Fisheries Science, National Taiwan University, Taipei, Taiwan
[5]Biology of Aquatic Organisms and Ecosystems (BOREA), Muséum National d'Histoire Naturelle, Sorbonne Université, CNRS, IRD, Paris, France
[6]Center of Excellence for the Oceans, National Taiwan Ocean University, Keelung, Taiwan

Received: 8 November 2024 / Accepted: 1 April 2025
Published online: 12 April 2025

References

1. Belcaid M, Casaburi G, McAnulty SJ, Schmidbaur H, Suria AM, Moriano-Gutierrez S, Pankey MS, Oakley TH, Kremer N, Koch EJ, Collins AJ, Nguyen H, et al. Symbiotic organs shaped by distinct modes of genome evolution in cephalopods. Proc Natl Acad Sci U S A. 2019;116:3030–5.
2. Nyholm SV, McFall-Ngai MJ. A lasting symbiosis: how the Hawaiian bobtail squid finds and keeps its bioluminescent bacterial partner. Nat Rev Microbiol. 2021;19:666–79.
3. Lum-Kong A. A histological study of the accessory reproductive organs of female *Loligo Forbesi* (Cephalopoda: Loliginidae). J Zool. 1992;226:469–90.
4. Huang JD, Lee SY, Chiang TY, Lu CC, Lee MF. Morphology of reproductive accessory glands in female *Sepia Pharaonis* (Cephalopoda: Sepiidae) sheds light on egg encapsulation. J Morphol. 2018;279:1120–31.
5. Kerwin AH, Gromek SM, Suria AM, Samples RM, Deoss DJ, O'Donnell K, et al. Shielding the next generation: symbiotic bacteria from a reproductive organ protect bobtail squid eggs from fungal fouling. mBio. 2019;10:e02379-19.
6. Kerwin AH, Nyholm SV. Symbiotic bacteria associated with a bobtail squid reproductive system are detectable in the environment, and stable in the host and developing eggs. Environ Microbiol. 2017;19:1463–75.
7. Kaufman MR, Ikeda Y, Patton C, van Dykhuizen G, Epel D. Bacterial symbionts colonize the accessory nidamental gland of the squid *Loligo opalescens* via horizontal transmission. Biol Bull. 1998;194:36–43.
8. Kerwin AH, McAnulty SJ, Nyholm SV. Development of the accessory nidamental gland and associated bacterial community in the Hawaiian bobtail squid, *Euprymna scolopes*. Biol Bull. 2021;240:205–18.
9. Li HW, Chen C, Kuo WL, Lin CJ, Chang CF, Wu GC. The characteristics and expression profile of transferrin in the accessory nidamental gland of the Bigfin reef squid during bacteria transmission. Sci Rep. 2019;9:20163.
10. Yang SH, Chen C, Hsieh YE, Yang SY, Li HW, Ching TY, Wang CH, Chang CF, Tang SL, Wu GC. Bacterial dynamics in the accessory nidamental gland of *Sepioteuthis Lessoniana* throughout maturation. Microbes Environ. 2021;36:ME21030.
11. Lindgren AR, Pankey MS, Hochberg FG, Oakley TH. A multi-gene phylogeny of cephalopoda supports convergent morphological evolution in association with multiple habitat shifts in the marine environment. BMC Evol Biol. 2012;12:129.
12. Vijayan N, McAnulty SJ, Sanchez G, Jolly J, Ikeda Y, Nishiguchi MK, Réveillac E, Gestal C, Spady BL, Li DH, Burford BP, Kerwin AH, et al. Evolutionary history influences the microbiomes of a female symbiotic reproductive organ in cephalopods. Appl Environ Microbiol. 2024;90:e0099023.
13. McAnulty SJ, Kerwin AH, Koch E, Nuttall B, Suria AM, Collins AJ, Schleicher TR, Rader BA, Nyholm SV. Failure to launch: development of a reproductive organ linked to symbiotic bacteria. mBio. 2023;14:e0213122.
14. Boettcher KJ, Ruby EG, McFall-Ngai MJ. Bioluminescence in the symbiotic squid *Euprymna scolopes* is controlled by a daily biological rhythm. J Comp Physiol A. 1996;179:65–73.
15. Lupp C, Urbanowski M, Greenberg EP, Ruby EG. The *Vibrio fischeri* quorum-sensing systems Ain and Lux sequentially induce luminescence gene expression and are important for persistence in the squid host. Mol Microbiol. 2003;50:319–31.
16. Li HW, Kuo WL, Chen C, Tseng YC, Chang CF, Wu GC. The characteristics and expression profile of peptidoglycan recognition protein 2 in the accessory nidamental gland of the Bigfin reef squid during bacterial colonization. Front Mar Sci. 2022;9:20163.
17. Lum-Kong A, Hastings TS. The accessory nidamental glands of *Loligo Forbesi* (Cephalopoda: Loliginidae): characterization of symbiotic bacteria and preliminary experiments to investigate factors controlling sexual maturation. J Zool. 1992;228:395–403.
18. Van den Branden C, Gillis M, Richard A. Carotenoid producing bacteria in the accessory Nidaental glands of *Sepia officinalis* L. Comp Biochem Physiol B Comp Biochem. 1980;66:331–4.
19. Dieser M, Greenwood M, Foreman CM. Carotenoid pigmentation in Antarctic heterotrophic bacteria as a strategy to withstand environmental stresses. Arct Antarct Alp Res. 2010;42:396–405.
20. Asker D, Beppu T, Ueda K. Unique diversity of carotenoid-producing bacteria isolated from Misasa, a radioactive site in Japan. Appl Microbiol Biotechnol. 2007;77:383–92.
21. Mohammadi M, Burbank L, Roper MC. Biological role of pigment production for the bacterial phytopathogen *Pantoea Stewartii subsp. Stewartii*. Appl Environ Microbiol. 2012;78:6859–65.
22. Rutherford ST, Bassler BL. Bacterial quorum sensing: its role in virulence and possibilities for its control. Cold Spring Harb Perspect Med. 2012;2:a012427.
23. Gromek SM, Suria AM, Fullmer MS, Gracia JL, Peter Gogarten J, Nyholm SV, Balunas MJ. Bobtail squid eggs, produces indigoidine and differentially inhibits *Vibrios*. Front Microbiol. 2016;7:1342.
24. Chen C, Li HW, Ku WL, Lin CJ, Chang CF, Wu GC. Two distinct vitellogenin genes are similar in function and expression in the Bigfin reef squid *Sepioteuthis Lessoniana*. Biol Reprod. 2018;99:1034–44.
25. Folmer O, Black M, Hoeh W, Lutz R, Vrijenhoek R. DNA primers for amplification of mitochondrial cytochrome C oxidase subunit I from diverse metazoan invertebrates. Mol Mar Biol Biotechnol. 1994;3:294–9.
26. Nossa CW, Oberdorf WE, Yang L, Aas JA, Paster BJ, Desantis TZ, Brodie EL, Malamud D, Poles MA, Pei Z. Design of 16S rRNA gene primers for 454 pyrosequencing of the human foregut Microbiome. World J Gastroenterol. 2010;16:4135–44.
27. Ram S, Mitra M, Shah F, Tirkey SR, Mishra S. Bacteria as an alternate biofactory for carotenoid production: A review of its applications, opportunities and challenges. J Funct Foods. 2020;67:103867.
28. Achenbach H, Kohl W, Wachter W, Reichenbach H. Investigations of the pigments from *Cytophaga Johnsonae* Cy Jl. new flexirubin-type pigments. Arch Microbiol. 1978;117:253–7.
29. Bowman. Out from the shadows - Resolution of the taxonomy of the family Cryomorphaceae. Front Microbiol. 2020;11:795.
30. Collins AJ, Schleicher TR, Rader BA, Nyholm SV. Understanding the role of host hemocytes in a squid/*Vibrio* symbiosis using transcriptomics and proteomics. Front Immunol. 2012;3:91.
31. Solis AG, Klapholz M, Zhao J, Levy M. The bidirectional nature of microbiome-epithelial cell interactions. Curr Opin Microbiol. 2020;56:45–51.
32. Wang RX, Lee JS, Campbell EL, Colgan SP. Microbiota-derived butyrate dynamically regulates intestinal homeostasis through regulation of actin-associated protein Synaptopodin. Proc Natl Acad Sci U S A. 2020;117:11648–57.

33. Mathieu E, Escribano-Vazquez U, Descamps D, Cherbuy C, Langella P, Riffault S, Remot A, Thomas M. Paradigms of lung microbiota functions in health and disease, particularly, in asthma. Front Physiol. 2018;9:1168.
34. Tseng PW, Li HW, Chen C, Tseng YC, Chang CF, Wu GC. Transcriptomic profile of symbiotic accessory nidamental gland during female maturation in Bigfin reef squid. Front Mar Sci. 2023;9:1026742.
35. Alex S, Lange K, Amolo T, Grinstead JS, Haakonsson AK, Szalowska E, Koppen A, Mudde K, Haenen D, Al-Lahham S, Roelofsen H, Houtman R, et al. Short-chain fatty acids stimulate angiopoietin-like 4 synthesis in human colon adenocarcinoma cells by activating peroxisome proliferator-activated receptor γ. Mol Cell Biol. 2013;33:1303–16.
36. Byndloss MX, Olsan EE, Rivera-Chávez F, Tiffany CR, Cevallos SA, Lokken KL, Torres TP, Byndloss AJ, Faber F, Gao Y, Litvak Y, Lopez CA, et al. Microbiota-activated PPAR-γ signaling inhibits dysbiotic *Enterobacteriaceae* expansion. Science. 2017;357:570–5.
37. Hinzke T, Kleiner M, Breusing C, Felbeck H, Häsler R, Sievert SM, Schlüter R, Rosenstiel P, Reusch TBH, Schweder T, Markert S. Host-Microbe interactions in the chemosynthetic *Riftia pachyptila* symbiosis. mBio. 2019;10:e02243–19.
38. Ponnudurai R, Kleiner M, Sayavedra L, Petersen JM, Moche M, Otto A, Becher D, Takeuchi T, Satoh N, Dubilier N, Schweder T, Markert S. Metabolic and physiological interdependencies in the *Bathymodiolus azoricus* symbiosis. Isme J. 2017;11:463–77.
39. Gestal C, Castellanos-Martínez S. Understanding the cephalopod immune system based on functional and molecular evidence. Fish Shellfish Immunol. 2015;46:120–30.
40. Troll JV, Bent EH, Pacquette N, Wier AM, Goldman WE, Silverman N, McFall-Ngai MJ. Taming the symbiont for coexistence: a host PGRP neutralizes a bacterial symbiont toxin. Environ Microbiol. 2010;12:2190–203.

Publisher's note